

Self-Sensing Composites and Optimization of Composite Structures in Japan

Akira Todoroki*

*Department of Mechanical Sciences and Engineering, Tokyo Institute of Technology, 2-12-1 Ookayama, Meguro, Tokyo, Japan
1528552*

Abstract

I review research on self-sensing and structural optimizations of laminated carbon/epoxy composites in Japan. Self-sensing is one of the multiple functions of composites; i.e., carbon fiber is used as a sensor as well as reinforcement. I present a controversial issue in self-sensing and detail research results. Structural optimization of laminated CFRP composites is indispensable in reducing the weights of modern aerospace structural components. I present a modified efficient global search method using the multi-objective genetic algorithm and fractal branch and bound method. My group has focused its research on these subjects and our research results are presented here.

Key words: Laminated composites, Self-sensing, Optimization, Damage

1. Introduction

Since laminated carbon fiber reinforced polymer (CFRP) composites have high specific strength and stiffness, they can be effectively used to reduce the weights of aeronautical structural components. Laminated CFRP is made from unidirectional prepreg or a woven fabric sheet. The laminated composite structures used in aerospace engineering require the design of the stacking sequence as well as the design of dimensions because the mechanical properties of the laminated components strongly depend on the stacking sequence of the laminates. Many aircraft composite structures are designed using the building block approach of MIL-Handbook-17. The building block approach requires a large number of experiments, which limits the available fiber orientations to a small set of 0°, 45°, -45° and 90° to prevent high experimental cost. Therefore, optimization of the stacking sequence is combinatorial optimization with a limited number of available fiber angles.

It is difficult to detect internal damage to a laminated CFRP structure such as delamination or matrix cracking because

such damage is not visible at the exterior of the structure. The inability to inspect CFRP structures visually demands the development of automatic monitoring or damage-detection systems. Although fiber optic sensors are good candidates as damage-monitoring sensors, they require further research before they can be considered to be effective. Carbon fiber is an excellent electrical conductor and has been used as a strain sensor for decades. One possible damage/strain sensing method for CFRP composites is self-sensing using carbon fibers as sensors.

In the present study, the self-sensing of CFRP composites and the structural optimization of CFRP components in Japan are reviewed. Recent research on self-sensing has achieved identification of the damage location and dimensions through measurement of changes in the electrical resistance at multiple points within target CFRP structures. This paper reviews some of the significant research to have been carried out in Japan. The optimization of composites is then reviewed to provide clear solutions to problems of design methods of laminated CFRP; i.e., simultaneous optimizations of stacking sequences and dimensions of stiffened panels.

©* Professor, Corresponding author
E-mail: atodorok@ginza.mes.titech.ac.jp Tel: +81-3-5734-3178

2. Self-Sensing CFRP Composites

2.1 Introduction

Carbon fiber is an electrically conductive material. Even in the direction transverse to the fiber direction, electric current flows because of fiber contact. Delamination cracks and matrix cracking of CFRP composites can be detected through measurements of changes in the electrical resistance. This damage detection technique does not require additional sensors; the reinforcement carbon fibers are used as sensors. Hence, the method of measuring the electrical resistance change of CFRP composites is referred to as a self-sensing method.

Self-sensing CFRP is a multifunctional composite. The present review presents research on self-sensing CFRP in Japan.

2.2 Piezoresistivity

Employing a two-probe method, Schulte and Baron (1989) reported that the electrical resistance of a CFRP laminate in the fiber direction increases as the tensile load applied in the fiber direction increases. The two-probe method applies two electrodes to measure the electrical resistance as shown in Fig. 1. Other researchers also reported this positive piezoresistance (a positive gage factor) (Ceysson et al., 1996; Irving and Thiagarajan, 1998; Muto et al., 1993; Xu et al., 1996).

Wang and Chung (2000) obtained contrary results. They employed a four-probe method to measure the precise change in electrical resistance in the fiber direction during tensile loading in the fiber direction of a CFRP laminate as shown in Fig. 2. Their results showed negative piezoresistance (a negative gage factor.) The electrical resistance in the fiber direction decreases with an increase in the tensile load applied in the fiber direction (see Fig. 3). The four-probe

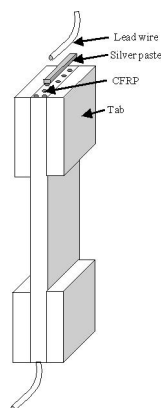


Fig. 1. Typical two-probe method.

method uses an outer pair of electrodes to apply electric current and an inner pair of electrodes to measure the resistance from the voltage drop between the pairs.

On the other hand, Ogi and Takao (2005) experimentally showed positive piezoresistivity of unidirectional CFRP using the four-probe method. They presented a significant model of the piezoresistivity of unidirectional CFRP. Todoroki and Yoshida (2004) also revealed experimentally that the unidirectional CFRP has positive piezoresistivity using the four-probe method. In the experiments (Todoroki and Yoshida, 2004), negative piezoresistivity was obtained before removing the surface resin without polishing the surface. In a test using an identical specimen, the surface was polished and positive piezoresistivity was obtained. The results are shown in Figs. 4 and 5. In these figures, the abscissa is the applied tensile strain and the ordinate is the ratio of electrical resistance change. The figures show that electrical contact at the electrodes affects the resistance change. Angelidis et al. (2004) and Todoroki and Yoshida (2005) showed that the electrical contact at the electric-current electrodes affects the measurement of the electrical resistance of CFRP.

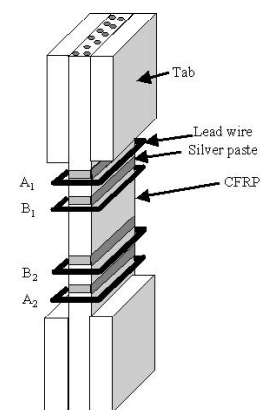


Fig. 2. Typical four-probe method.

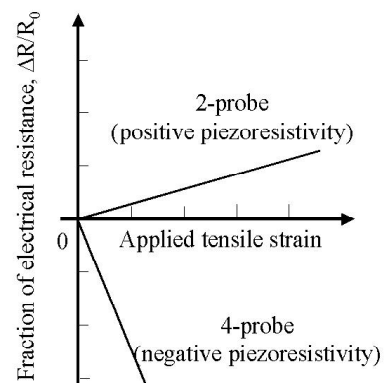


Fig. 3. Discrepancy between the two-probe method and four-probe method.

Even if we use the four-probe method, the strongly orthotropic conductivity of CFRP causes a problem of electrical contact at the electrodes where applying electric current. In the case of the self-sensing CFRP, electrical contact at the electrodes is quite significant even if we use the four-probe method. A method using electrodes made of electrical copper plating is presented in the other paper along with tests results of durability (Todoroki et al., 2010c).

2.3 Monitoring of fiber breakages and matrix cracking

Self-sensing methods have been applied to fatigue damage detection by several researchers (Muto et al., 1993; Seo and Lee, 1999). All applied processes are similar to the monotonic tensile test to measure the change in electrical resistance in CFRP specimens. These tests were applied to unidirectional CFRP and cross-ply CFRP laminates. The electrical resistance increased with a decrease in specimen stiffness. The increase in the electrical resistance of the unidirectional CFRP indicates that the self-sensing method

detects fiber breakages.

Park et al. (2001) and Xia et al. (2003) proposed an interesting model of carbon fiber networks to simulate the gradual increase in the electrical resistance of CFRP under tensile loading. They modeled the CFRP as a network of resistances and found several required properties of the model through comparison with experimental data.

Omagari et al. (2005), Todoroki and Omagari (2008), and Todoroki et al. (2006a, b) showed that the four-probe method is applicable to the monitoring of matrix cracking in cross-ply CFRP laminates. In their tests, four probes were placed on a single surface of a beam specimen as shown in Fig. 6.

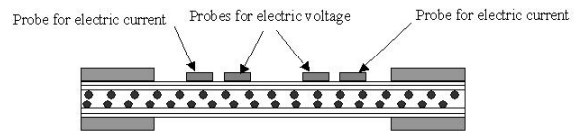


Fig. 6. Schematic representation of the self-sensing method employed to detect matrix cracking (Todoroki et al., 2006a).

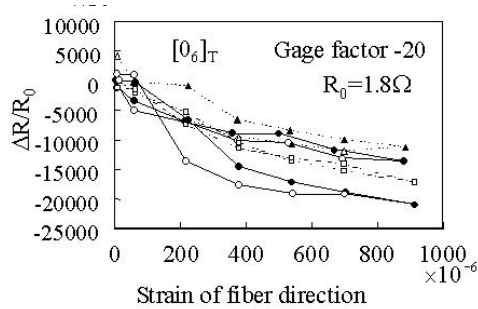


Fig. 4. Measured piezoresistance for a test tensile load applied in the fiber direction and electrical resistance measured in the fiber direction without polishing the specimen surface as reported by Todoroki and Yoshida (2004). (Solid symbols represent loading and open symbols unloading.)

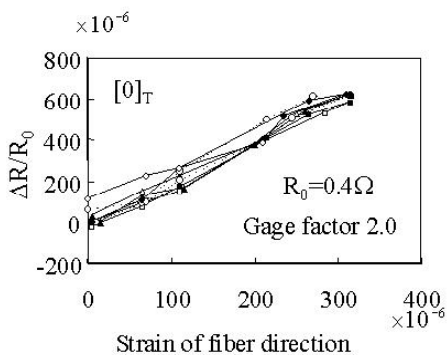


Fig. 5. Piezoresistance of a small zero-tensile-zero-charge single-ply specimen measured by Todoroki and Yoshida (2004). (Solid symbols represent loading and open symbols unloading.)

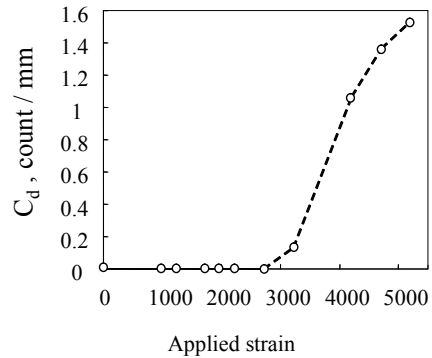


Fig. 7. Matrix crack density measured employing a replica method (Todoroki et al., 2006a).

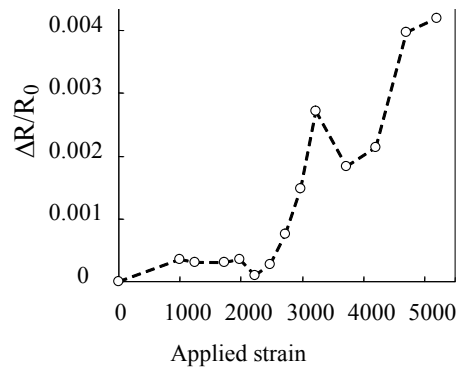


Fig. 8. Measured residual change in electrical resistance of a cross-ply carbon fiber reinforced polymer under a completely unloading condition plotted against the maximum applied strain (Todoroki et al., 2006a).

Tensile tests were then performed to measure the density of matrix cracks; the measured density is shown in Fig. 7. The electrical resistance measured under a completely unloading condition is shown in Fig. 8. The experimental results reveal that electrical resistance increased with matrix cracking. Even after complete unloading, specimens with matrix cracks retained a residual increase in electrical resistance. The effect of specimen thickness on the residual electrical resistance increase was also investigated. When 90° ply is thicker than 0° ply, the effect of residual stress relief is smaller, and this causes the crack surface contact. Therefore, the slope of the plot of the fraction of the electrical resistance change versus reloading during reloading has been considered. The method was also employed to investigate damage at cryogenic temperatures (Todoroki et al., 2006b) and found to work well in detecting the initiation of damage even at such temperatures.

2.4 Monitoring of delamination

The self-sensing method based on the change in electrical resistance has been applied in monitoring delamination cracking. Since electrical resistance changes due to delamination cracking are very small, Hirano and Todoroki (2007), Todoroki (2001), Todoroki et al. (2002a, b, 2003, 2004a, b, 2005, 2010a, b), Todoroki and Suzuki (2000), Todoroki and Tanaka (2002), Ueda and Todoroki (2006, 2008), and Ueda et al. (2004, 2005) applied an electrical bridge circuit or modified amplifiers to obtain large output signals from the delamination events. The modified bridge circuit is schematically shown in Fig. 9. Since this only differs from the bridge circuit in a conventional strain gage by a connected electrical resistance, a conventional strain amplifier can be directly applied without modification of the circuit. Moreover, as for conventional strain gages, temperature compensation is possible using a dummy specimen.

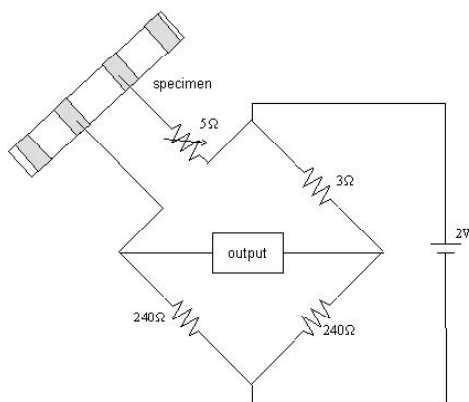


Fig. 9. Schematic representation of a modified electrical bridge circuit (Todoroki and Tanaka, 2002).

In the monitoring, Hirano and Todoroki (2007), Todoroki (2001), Todoroki and Suzuki (2000), Todoroki et al. (2002a, b, 2003, 2004a, b, 2005), Todoroki and Tanaka (2002), Ueda and Todoroki (2006, 2008), and Ueda et al. (2004, 2005) used response surfaces to obtain the relationship between the electrical resistance changes and delamination location or dimensions. Quadratic polynomials were adopted because of their simplicity. The response surface can be described with quadratic polynomials as follows.

$$y = \beta_0 + \sum_{j=1}^k \beta_j x_j + \sum_{j=1}^k \beta_{jj} x_j^2 + \sum_{i=1}^{k-1} \sum_{j=i+1}^k \beta_{ij} x_i x_j \quad (1)$$

Although the method requires a large number of experiments, it does not demand modeling. Instead of the experiments, finite-element method (FEM) analyses can be carried out to obtain electrical resistance changes due to delamination cracking (Todoroki et al., 2010a, b).

The method based on the change in electrical resistance has also been applied to plate-type specimens (Todoroki et al., 2002b). An example of the configuration of these specimens is shown in Fig. 10. In this example, 10 electrodes were co-cured onto the plate to measure changes in the electrical resistance (copper plating can be used for existing structures). Delamination was achieved by indentation loading with a cylindrical jig. The delamination location and dimensions were estimated on the basis of the response surface. The delamination was estimated for both cross-ply and quasi-isotropic laminates. Figure 11 shows the typical estimation results for the delamination location (*x*-coordinate). The abscissa is the measured delamination location and the ordinate is the estimated delamination location. Figure 12 shows typical estimation results for the delamination size.

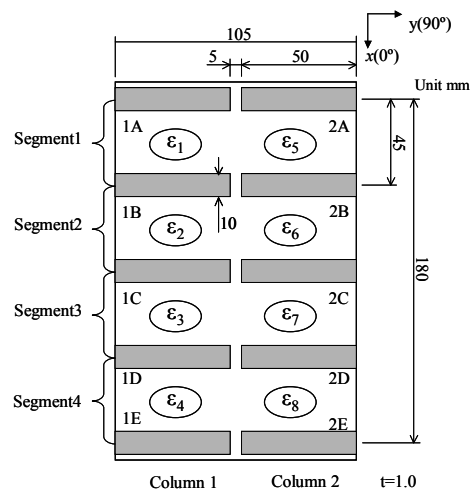


Fig. 10. Schematic representation of the configuration of a plate-type specimen (Todoroki et al., 2002b).

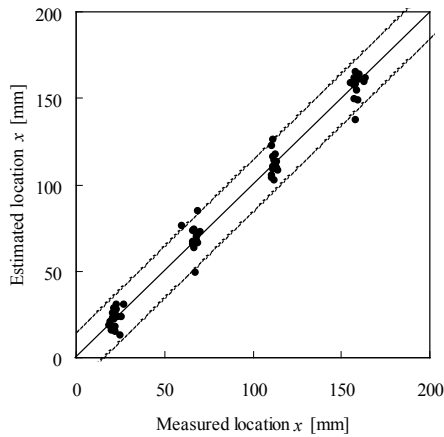


Fig. 11. Typical monitoring of the location of delamination of cross-ply plates.

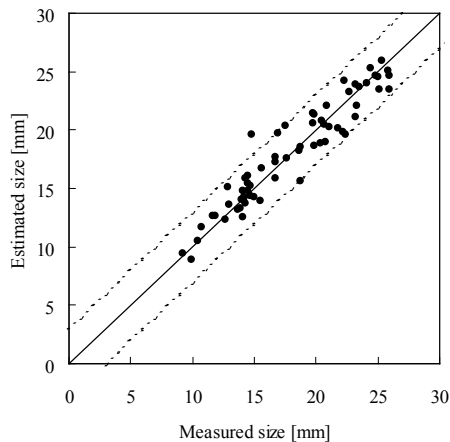


Fig. 12. Typical monitoring of the location of delamination of cross-ply plates.

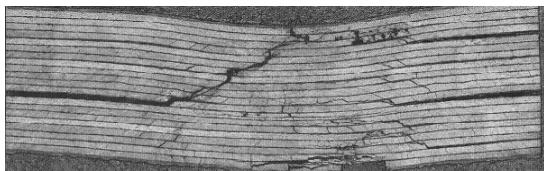


Fig. 13. Typical delamination with a dent.

The abscissa is the measured maximum size of delamination and the ordinate is the estimated results. The estimates of the delamination size and location were quite accurate as shown in the figures. In estimating the delamination location and size, the estimation results for the quasi-isotropic laminate were also very good when normalized electrical resistance changes were used (Todoroki et al., 2003).

The estimation method requires a large number of experiments to make the response surfaces. FEM analyses allow the number of experiments to be reduced for thin CFRP

laminates (Todoroki et al., 2010b). However, delamination decreases the electrical resistance of thick CFRP laminates (Todoroki et al., 2010a) but increases the electrical resistance of a thin CFRP laminate (Todoroki et al., 2010b). For thick CFRP laminates, delamination results in a dent as shown in Fig. 13, which decreases the electrical resistance of a thick CFRP laminate.

The durability of electrodes was tested by Todoroki et al. (2010c). The self-sensing method has also been applied to detect compression damage such as fiber microbuckling (Todoroki et al., 2010d). In addition, bolted joint damage has been monitored employing the method (Shimamura et al., 2006).

3. Structural Optimization of Laminated Composites

3.1 Introduction

The use of laminated composite structures in aerospace engineering requires the design of the stacking sequence as well as the dimensions because the mechanical properties of the laminated components strongly depend on the stacking sequences of the laminates. Many aircraft composite structures are designed using the building block approach of MIL-Handbook-17. The building block approach requires a large number of experiments, and this limits the available fiber orientations to a small set of 0° , 45° , -45° and 90° to prevent high experimental cost. Hence, the stacking sequence optimization is a combinatorial optimization with limited fiber angles as previously mentioned.

For the stacking sequence optimizations, Miki (1985) and Fukunaga and Chou (1988) proposed a graphical optimization method employing lamination parameters. Genetic algorithms are widely used to optimize the stacking sequence (Cho and Rhee, 2003; Kogiso et al., 1994; Le Riche and Haftka, 1993; Liu et al., 2000; Marcellin et al., 1995; Todoroki and Haftka, 1998; Todoroki and Sasai, 1999; Todoroki et al., 1995; Zako et al., 1997). Narita (2003) proposed a layer-wise optimization method, which has the lowest computational cost.

Terada et al. (2001) and Todoroki and Terada (2004) published a new deterministic method for the optimization of the stacking sequence of composite laminates, named the fractal branch and bound (FBB) method. The FBB method has been applied to maximization problems of buckling load (Terada et al., 2001; Todoroki and Terada, 2004). The FBB method has also been applied to maximization problems of the flutter speed of a laminated composite wing that has multiple local maxima (Hirano and Todoroki, 2004, 2005).

The FBB method has been extended to the simultaneous optimization of the stacking sequence of multiple laminates, such as laminates of a stiffened panel (Sekishiro and Todoroki, 2006; Todoroki and Sekishiro, 2007), and to asymmetrical laminates (Matsuzaki and Todoroki, 2007).

In optimizing composite structures, Yamazaki (1996) employed a well-known mathematical programming method for stiffened composite components with lamination parameters. The lamination parameters are considered as independent design variables in the first stage. In the second stage, practical stacking sequences that have lamination parameters similar to those of the optimal sets are searched using a genetic algorithm.

The present review focuses on the modified efficient global optimization method (Todoroki and Sekishiro, 2008a, b) using the FBB and multi-objective genetic algorithm (MOGA). The method optimizes the stacking sequences and dimensions of a stiffened composite panel simultaneously. The FBB for multiple laminates is integrated in the new method as a lower-layer optimization.

3.2 Lamination parameters

In-plane stiffness terms of symmetric laminates are represented with in-plane lamination parameters V_i^* as follows.

$$\begin{bmatrix} A_{11} \\ A_{22} \\ A_{12} \\ A_{66} \\ A_{16} \\ A_{26} \end{bmatrix} = h \begin{bmatrix} U_1 & V_1^* & V_2^* \\ U_1 & -V_1^* & V_2^* \\ U_4 & 0 & -V_2^* \\ U_5 & 0 & -V_2^* \\ 0 & \frac{1}{2}V_3^* & V_4^* \\ 0 & \frac{1}{2}V_3^* & -V_4^* \end{bmatrix} \begin{bmatrix} 1 \\ U_2 \\ U_3 \end{bmatrix} \quad (2)$$

Here h is the thickness of the laminate, U_i ($i = 1, \dots, 5$) denotes the material invariants, and V_i^* denotes the in-plane lamination parameters. The material invariants are as follows.

$$\begin{aligned} U_1 &= \frac{1}{8}(3Q_{11} + 3Q_{22} + 2Q_{12} + 4Q_{66}) \\ U_2 &= \frac{1}{2}(Q_{11} - Q_{22}) \\ U_3 &= \frac{1}{8}(Q_{11} + Q_{22} - 2Q_{12} - 4Q_{66}) \end{aligned} \quad (3)$$

$$\text{Here, } \begin{aligned} U_4 &= \frac{1}{8}(Q_{11} + Q_{22} + 6Q_{12} - 4Q_{66}) \\ Q_{11} &= \frac{E_L}{1 - \nu_{LT}\nu_{TL}}, & Q_{22} &= \frac{E_T}{1 - \nu_{LT}\nu_{TL}}, \\ Q_{12} &= \frac{\nu_{LT}E_T}{1 - \nu_{LT}\nu_{TL}}, & Q_{66} &= G_{LT}, \end{aligned} \quad (4)$$

where E_L is elastic modulus in the fiber direction, E_T is elastic modulus in the transverse direction, ν_{LT} is the major

Poisson ratio, and G_{LT} is the shear modulus.

The in-plane lamination parameters are as follows.

$$\mathbf{v} = \begin{bmatrix} V_1^* \\ V_2^* \\ V_3^* \\ V_4^* \end{bmatrix} = \frac{2}{h} \int_0^{h/2} \begin{bmatrix} \cos 2\theta \\ \cos 4\theta \\ \sin 2\theta \\ \sin 4\theta \end{bmatrix} dz \quad (5)$$

Here z is the coordinate of the thickness direction, the origin is at the middle of the plate, and $\theta(z)$ is the fiber angle at location z .

The out-of-plane stiffness terms of the laminates are represented with out-of-plane lamination parameters W_i^* as follows.

$$\begin{bmatrix} D_{11} \\ D_{22} \\ D_{12} \\ D_{66} \\ D_{16} \\ D_{26} \end{bmatrix} = \frac{h^3}{12} \begin{bmatrix} U_1 & W_1^* & W_2^* \\ U_1 & -W_1^* & W_2^* \\ U_4 & 0 & -W_2^* \\ U_5 & 0 & -W_2^* \\ 0 & \frac{1}{2}W_3^* & W_4^* \\ 0 & \frac{1}{2}W_3^* & -W_4^* \end{bmatrix} \begin{bmatrix} 1 \\ U_2 \\ U_3 \end{bmatrix} \quad (6)$$

The out-of-plane lamination parameters are defined as follows.

$$\mathbf{w} = \begin{bmatrix} W_1^* \\ W_2^* \\ W_3^* \\ W_4^* \end{bmatrix} = \frac{24}{h^3} \int_0^{h/2} z^2 \begin{bmatrix} \cos 2\theta(z) \\ \cos 4\theta(z) \\ \sin 2\theta(z) \\ \sin 4\theta(z) \end{bmatrix} dz \quad (7)$$

Plots of all feasible laminates in the lamination parameter space are fractal images when the fiber angles are limited to small sets (Todoroki and Terada, 2004). The FBB method uses the branch-and-bound method to prune the inferior branches using a surrogate model of a quadratic response surface.

3.3 Optimization problem

The optimization target is a blade-stiffened composite panel as shown in Fig. 14. The design variables of the stiffener are a height of the stiffener of h , width of the blade base of b_s , spacing between the blades of s , total number of plies of the panel N_p , and number of plies of the blade stiffener N_s . The length of the panel is fixed at $a = 0.25$ m and the width of the blade-stiffened panel at $b = 0.16$ m.

The buckling load is defined as the ratio (λ) of the buckling load to the single-compression load along the x -axis using commercially available finite element method (FEM) code ANSYS; the load is $N_x = 15,000$ kN/m. In the linear FEM analyses adopted here, 8-node linear shell elements (SHELL99) are used; the total number of elements is 3,000 and the total number of nodes is 10,000. The boundary condition of the FEM analysis in the y -direction is a repeating

structure as shown in Fig. 14; the edges of the y -axis are free but there is no rotation around the x -axis. The edges of loading (x -axis) are fixed grip. This optimization problem is expressed as follows.

$$\begin{aligned} &\text{minimize } W \\ &\text{subject to } \lambda \geq 1 \end{aligned} \tag{8}$$

The total weight of the blade-stiffened panel is easily calculated as follows.

$$W = \{bt_p + 2(b_2 + h)t_s\}\rho a = \{bN_p + 2(b_2 + h)N_s\}\rho at_{ply} \tag{9}$$

Here $t = 2Nt_{ply}$, where t_{ply} is the thickness of a single ply.

In Eq. (8), the first constraint means that the buckling load must be greater than 15,000 kN/m. The available range of each design variable is given in Table 1.

The material used here is carbon-fiber-reinforced epoxy composite T300/5208. The material properties are presented in Table 2. The composite panel and blade-stiffener are symmetric laminates, and the available fiber angles are limited to a small set of four angles: 0° , $\pm 45^\circ$ and 90° . In the case of the fiber angles, there is a balance rule for the ply angles and a four-contiguous-ply rule to prevent large matrix cracking; i.e., no more than four plies with the same fiber angle can be stacked contiguously.

3.4 Optimization using the MOGA

The objective function of the optimization problem (Eq. [8]) is simple and easily calculated when all dimensions of the stiffened panel are given. However, determination of the buckling load constraint has large computational cost because it requires FEM analysis in each evaluation of the buckling load. Here, the objective function of Eq. (8) is directly used without the surrogate model. On the other hand, the constraint of the buckling load ratio is approximated using a Kriging model to reduce the computational cost. As the variables of the response surface, all dimensions of the blade-

stiffened panel and the lamination parameters of both panel and stiffener are adopted here. Since automatic construction of a Kriging model is useful, the design and analysis of computer experiments (DACE) model is employed (Welch et al., 1992).

The Kriging mode enables us to calculate the estimator of the standard deviation, and the value is used to calculate the estimation error. For the DACE model, the estimation errors at the sampling points are zero, and the estimation error becomes large when the estimation point is far from the adjacent sampling points.

Latin hypercube sampling (LHS) experiments are adopted here (Welch et al., 1992). LHS gives uniformly distributed sampling in the entire design space. However, LHS is not simple for composite structures because lamination parameters (Fukunaga and Chou, 1988; Miki, 1985) are not independent variables. To solve this problem, we prepared all feasible symmetric laminates of 16 plies (i.e., the half ply number is eight). The total number of feasible plies that satisfy the balancing rule is 3281. From this set of feasible laminates, a set of laminates (the number of laminates is n_s) is selected randomly with some constraints. The constraints are imposed on the in-plane lamination parameters.

To select candidate points for variables of dimensions, all variables are divided into n_s segments. Feasible design scopes of the variable are normalized from -1 to $+1$, and equal segmentations are adopted. The number of plies N must be a positive integer. This is achieved by rounding numbers. From these segmented variables, a table of all segments is constructed and equally distributed sampling points are obtained. FEM analyses are performed at all sampling points. Using the FEM analysis results, a Kriging model of the buckling load ratio is constructed. The total number of FEM analyses is $n_s = 251$.

The multi-objective genetic algorithm (MOGA) has already been published in a well-known textbook (Deb, 2001). Since

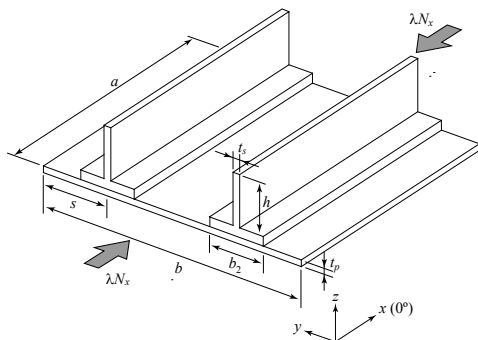


Fig. 14. Analysis model of the blade-stiffened panel.

Table 1. Design variables

Design variable	Min.	Max.
h	0.01	0.05
b_2	0.02	0.04
s	0.03	0.05
N_p	4	16
N_s	4	16

Table 2. Material properties of T300/5208

E_L	181 (GPa)
E_T	10.3 (GPa)
G_{LT}	7.17 (GPa)
ν_{LT}	0.28
ρ	$1.6 \times 10^3 \text{ kg/m}^3$

the MOGA is similar to a simple genetic algorithm, a detailed explanation is not given here.

The present method employs two-layer optimization. In the upper layer, the structural dimensions are optimized using the MOGA. Chromosomes of each individual correspond to structural dimensions such as the height or width of the stiffener, and these dimensions are sufficient information for evaluating the structural weight. To evaluate the buckling load, however, the stacking sequence of the composite laminates must be known. The upper-layer optimization activates a lower-layer optimization of the stacking sequence. The stacking sequence of the stiffener and panel are optimized employing the modified FBB method; this is a modified version of the FBB method that optimizes more than two laminates simultaneously. These optimization processes are described as follows.

- (1) The experiments are designed using the LHS to select n_s points. FEM analyses of the buckling load are conducted at the n_s selected points. A Kriging model is constructed from the results for the n_s points. There should be more than 10 times as many points as design variables. On the basis of the selected points, the minimum-weight structure that satisfies the buckling load constraint is selected as the provisional optimal structure (W_{min}).
- (2) Initial individuals of the MOGA (total population of 100) are determined using random numbers.
- (3) Upper-layer optimization is performed using the MOGA.
 - (a) The fitness of each individual is evaluated; lower-layer optimization is performed to optimize the stacking sequence of the stiffener and panel using the extended FBB method.
 - (b) Non-dominated individuals are searched using two objective functions: weight reduction relative to the provisional structure and the probability of satisfaction of the buckling load.
 - (c) The diversity of the population is evaluated for all individuals, and the fitness value of each individual is calculated.
 - (d) Selection is performed using a Parate-ranking method, and mutation conducted after crossover of the selected individuals.
- (4) The MOGA is terminated after the 300th generation.
- (5) The top 10 individuals of the probability of satisfaction of the buckling load are calculated employing FEM analyses with consideration of the diversity of the population in the 100 Parate solutions.

The 10 new FEM results are added to the Kriging model dataset. The process cycles from step (2).

3.5 Results and Discussion

A total of 251 points were selected in the LHS experiments, and FEM analyses were conducted at the selected sampling points. Cross-validations of the Kriging model were performed at all points, and the results are shown in Fig. 15. The cross-validation is the checking method of the Kriging model; a Kriging model is calculated from a set of sampling data except for a selected point, and the selected point is estimated with the calculated Kriging model. Afterward, the Kriging model is estimated at the selected point. Thus, all data shown in Fig. 15 are the new data for the Kriging model. The abscissa is the true value and the ordinate is the estimated value. Good estimations are plotted on the diagonal line. Figure 15 shows that the Kriging model almost always provides good estimations.

Using this Kriging model, the optimizations of the MOGA are cycled 10 times; 50 extra FEM analyses were added to the Kriging model for accuracy. Figure 16 shows the results of the minimum-weight history of the MOGA. The result at zero cycles is the provisional optimal structure. As shown in Fig. 16, the Parate solutions obtained from the MOGA always include solutions that have a high probability of satisfying the constraint of the buckling load.

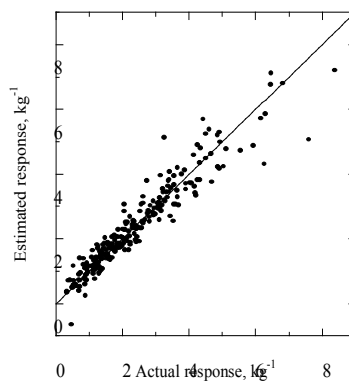


Fig. 15. Result of cross-validation of initial response surface.

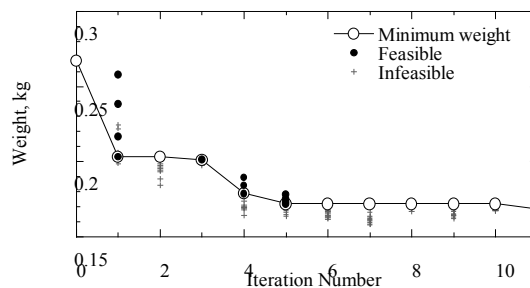


Fig. 16. Iteration history of the multi-objective genetic algorithm.

Table 3. Optimal design

W , kg	0.168
λ_b	1.00
h	0.0130
b_2	0.0345
s	0.0374
N_p	4
N_s	11
Panel	$[(\pm 45)_2]_S$
Stiffener	$[45/0_2/-45/0_4/90/0_2]_S$

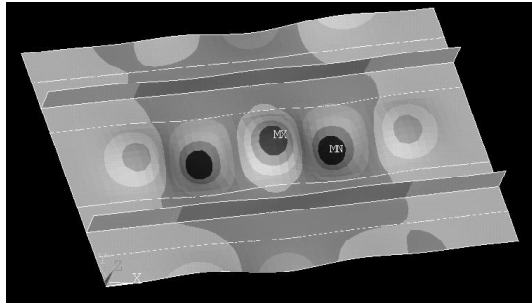


Fig. 17. Buckling mode of the optimized structure.

Table 3 gives the optimal solution obtained after five cycles of optimizations of the MOGA. In the optimizations of the MOGA, there were 361 FEM analyses. The obtained minimum weight is 0.168 kg. Figure 17 shows the buckling of the optimal designs. The result without optimization of the stacking sequence is 0.238 kg using fixed stacking sequences of quasi-isotropic laminates and the dimensions were selected as design variables in this case. The result obtained from the MOGA is 38% lighter than the result obtained without optimization of the stacking sequence.

The MOGA with the Kriging approximation and FBB method is adopted in the optimization of the dimensions of the stiffened panel and stacking sequences. Since the weight is easily calculated, only the constraint of the buckling load is approximated using a Kriging model named the DACE model. The new method is applied to a blade-stiffened panel to obtain the minimum-weight structure under a constraint of the buckling load. The results obtained show that the method provides a practically optimal result with relatively few FEM analyses.

4. Concluding Remarks

The present review covers the self-sensing and structural optimization of laminated carbon composites in Japan. The author's group has mainly researched these two areas. Self-sensing is one of the multiple functions of such composites. The self-sensing method has recently become popular because it does not require additional sensors. The

present review presents recent advances in self-sensing in the author's laboratory and a structural optimization method that optimizes the stacking sequence of laminated composites—a modified efficient global optimization method employing the MOGA. The review also presents the process of optimization and an optimization example of a blade-stiffened composite panel. The method significantly reduces the number of analyses required and provides a practical optimal result for reducing the weights of aerospace structural components.

References

- Angelidis, N., Wei, C. Y., and Irving, P. E. (2004). The electrical resistance response of continuous carbon fibre composite laminates to mechanical strain. *Composites Part A: Applied Science and Manufacturing*, 35, 1135-1147.
- Ceysson, O., Salvia, M., and Vincent, L. (1996). Damage mechanisms characterisation of carbon fibre/epoxy composite laminates by both electrical resistance measurements and acoustic emission analysis. *Scripta Materialia*, 34, 1273-1280.
- Cho, M. H. and Rhee, S. Y. (2003). Layup optimization considering free-edge strength and bounded uncertainty of material properties. *AIAA journal*, 41, 2274-2282.
- Deb, K. (2001). *Multi-Objective Optimization Using Evolutionary Algorithms*. 1st ed. Chichester: John Wiley & Sons.
- Fukunaga, H. and Chou, T.-W. (1988). Simplified design techniques for laminated cylindrical pressure vessels under stiffness and strength constraints. *Journal of Composite Materials*, 22, 1156-1169.
- Hirano, Y. and Todoroki, A. (2004). Stacking sequence optimizations for composite laminates using fractal branch and bound method: Application for supersonic panel flutter problem with buckling load condition. *Advanced Composite Materials: The Official Journal of the Japan Society of Composite Materials*, 13, 89-106.
- Hirano, Y. and Todoroki, A. (2005). Stacking-sequence optimization of composite delta wing to improve flutter limit using fractal branch and bound method. *JSME International Journal, Series A: Solid Mechanics and Material Engineering*, 48, 65-72.
- Hirano, Y. and Todoroki, A. (2007). Damage identification of woven graphite/epoxy composite beams using the electrical resistance change method. *Journal of Intelligent Material Systems and Structures*, 18, 253-263.
- Irving, P. E. and Thiagarajan, C. (1998). Fatigue damage characterization in carbon fibre composite materials using

an electrical potential technique. *Smart Materials and Structures*, 7, 456-466.

Kogiso, N., Watson, L. T., Gürdal, Z., and Haftka, R. T. (1994). Genetic algorithms with local improvement for composite laminate design. *Structural Optimization*, 7, 207-218.

Le Riche, R. and Haftka, R. T. (1993). Optimization of laminate stacking sequence for buckling load maximization by generic algorithm. *AIAA journal*, 31, 951-956.

Liu, B., T. Haftka, R., A. Akgün, M., and Todoroki, A. (2000). Permutation genetic algorithm for stacking sequence design of composite laminates. *Computer Methods in Applied Mechanics and Engineering*, 186, 357-372.

Marcelin, J. L., Trompette, P., and Dornberger, R. (1995). Optimal structural damping of skis using a genetic algorithm. *Structural Optimization*, 10, 67-70.

Matsuzaki, R. and Todoroki, A. (2007). Stacking-sequence optimization using fractal branch-and-bound method for unsymmetrical laminates. *Composite Structures*, 78, 537-550.

Miki, M. (1985). Design of laminated fibrous composite plates with required flexural stiffness. In J. R. Vinson and M. Taya, eds. *Recent Advances in Composites in the United States and Japan*. West Conshohocken, PA: American Society for Testing and Materials (ASTM) International. pp. 387-400.

Muto, N., Yanagida, H., Nakatsuji, T., Sugita, M., and Ohtsuka, Y. (1993). Preventing fatal fractures in carbon-fiber-glass-fiber-reinforced plastic composites by monitoring change in electrical resistance. *Journal of the American Ceramic Society*, 76, 875-879.

Narita, Y. (2003). Layerwise optimization for the maximum fundamental frequency of laminated composite plates. *Journal of Sound and Vibration*, 263, 1005-1016.

Ogi, K. and Takao, Y. (2005). Characterization of piezoresistance behavior in a CFRP unidirectional laminate. *Composites Science and Technology*, 65, 231-239.

Omagari, K., Todoroki, A., Shimamura, Y., and Kobayashi, H. (2005). Detection of matrix cracking of CFRP using electrical resistance changes. *Key Engineering Materials*, 297-300, 2096-2101.

Park, J. B., Okabe, T., Takeda, N., and Curtin, W. A. (2001). Electromechanical modeling of unidirectional CFRP composites under tensile loading condition. *Composites - Part A: Applied Science and Manufacturing*, 33, 267-275.

Schulte, K. and Baron, C. (1989). Load and failure analyses of CFRP laminates by means of electrical resistivity measurements. *Composites Science and Technology*, 36, 63-76.

Sekishiro, M. and Todoroki, A. (2006). Extended fractal branch and bound method for optimization of multiple

stacking sequences of stiffened composite panel. *Advanced Composite Materials: The Official Journal of the Japan Society of Composite Materials*, 15, 341-356.

Seo, D. C. and Lee, J. J. (1999). Damage detection of CFRP laminates using electrical resistance measurement and neural network. *Composite Structures*, 47, 525-530.

Shimamura, Y., Oda, K., Todoroki, A., and Ueda, M. (2006). Detectability of bearing failure of composite bolted joints by electric resistance change method. *Key Engineering Materials*, 321-323, 957-962.

Terada, Y., Todoroki, A., and Shimamura, Y. (2001). Stacking sequence optimizations using fractal branch and bound method for. *JSME International Journal, Series A: Solid Mechanics and Material Engineering*, 44, 490-498.

Todoroki, A. (2001). The effect of number of electrodes and diagnostic tool for monitoring the delamination of CFRP laminates by changes in electrical resistance. *Composites Science and Technology*, 61, 1871-1880.

Todoroki, A. and Haftka, R. T. (1998). Stacking sequence optimization by a genetic algorithm with a new recessive gene like repair strategy. *Composites Part B: Engineering*, 29, 277-285.

Todoroki, A. and Omagari, K. (2008). Detection of matrix crack density of CFRP using an electrical potential change method with multiple probes. *Journal of Solid Mechanics and Materials Engineering*, 2, 718-729.

Todoroki, A., Omagari, K., Shimamura, Y., and Kobayashi, H. (2006a). Matrix crack detection of CFRP using electrical resistance change with integrated surface probes. *Composites Science and Technology*, 66, 1539-1545.

Todoroki, A., Omagari, K., and Ueda, M. (2006b). Matrix crack detection of CFRP laminates in cryogenic temperature using electrical resistance change method. *Key Engineering Materials*, 321-323, 873-876.

Todoroki, A., Samejima, Y., Hirano, Y., Matsuzaki, R., and Mizutani, Y. (2010a). Electrical resistance change of thick CFRP laminate for self-sensing. *Journal of Solid Mechanics and Materials Engineering*, 4, 658-668.

Todoroki, A., Samejima, Y., Hirano, Y., Matsuzaki, R., and Mizutani, Y. (2010b). Mechanism of electrical resistance change of a thin CFRP beam after delamination cracking. *Journal of Solid Mechanics and Materials Engineering*, 4, 1-11.

Todoroki, A. and Sasai, M. (1999). Improvement of design reliability for buckling load maximization of composite cylinder using genetic algorithm with recessive-gene-like repair. *JSME International Journal, Series A: Solid Mechanics and Material Engineering*, 42, 530-536.

Todoroki, A. and Sekishiro, M. (2007). New iteration fractal branch and bound method for stacking sequence

optimizations of multiple laminates. *Composite Structures*, 81, 419-426.

Todoroki, A. and Sekishiro, M. (2008a). Modified efficient global optimization for a hat-stiffened composite panel with buckling constraint. *AIAA journal*, 46, 2257-2264.

Todoroki, A. and Sekishiro, M. (2008b). Optimization of blade stiffened composite panel under buckling and strength constraints. *Journal of Computational Science and Technology*, 2, 234-245.

Todoroki, A. and Suzuki, H. (2000). Health monitoring of internal delamination cracks for graphite/epoxy by electric potential method. *Applied Mechanics and Engineering*, 5, 283-294.

Todoroki, A., Suzuki, K., Mizutani, Y., and Matsuzaki, R. (2010c). Durability estimates of copper plated electrodes for self-sensing CFRP composites. *Journal of Solid Mechanics and Materials Engineering*, 4, 610-620.

Todoroki, A., Suzuki, K., Mizutani, Y., and Matsuzaki, R. (2010d). Electrical resistance change of CFRP under a compression load. *Journal of Solid Mechanics and Materials Engineering*, 4, 864-874.

Todoroki, A., Tanaka, M., and Shimamura, Y. (2002a). Measurement of orthotropic electric conductance of CFRP laminates and analysis of the effect on delamination monitoring with an electric resistance change method. *Composites Science and Technology*, 62, 619-628.

Todoroki, A., Tanaka, M., and Shimamura, Y. (2003). High performance estimations of delamination of graphite/epoxy laminates with electric resistance change method. *Composites Science and Technology*, 63, 1911-1920.

Todoroki, A., Tanaka, M., and Shimamura, Y. (2005). Electrical resistance change method for monitoring delaminations of CFRP laminates: Effect of spacing between electrodes. *Composites Science and Technology*, 65, 37-46.

Todoroki, A., Tanaka, M., Shimamura, Y., and Kobayashi, H. (2004a). Effects with a matrix crack on monitoring by electrical resistance method. *Advanced Composite Materials*, 13, 107-120.

Todoroki, A. and Tanaka, Y. (2002). Delamination identification of cross-ply graphite/epoxy composite beams using electric resistance change method. *Composites Science and Technology*, 62, 629-639.

Todoroki, A., Tanaka, Y., and Shimamura, Y. (2002b). Delamination monitoring of graphite/epoxy laminated composite plate of electric resistance change method. *Composites Science and Technology*, 62, 1151-1160.

Todoroki, A., Tanaka, Y., and Shimamura, Y. (2004b). Identifying Delamination in Cross-ply and Quasi-isotropic Beams of CFRP by a Standardized Electrical Resistance Method. *Polymers and Polymer Composites*, 12, 75-85.

Todoroki, A. and Terada, Y. (2004). Improved fractal branch and bound method for stacking-sequence optimizations of laminates. *AIAA journal*, 42, 141-148.

Todoroki, A., Watanabe, K., and Kobayashi, H. (1995). Application of genetic algorithms to stiffness optimization of laminated composite plates with stress-concentrated open holes. *JSME International Journal, Series A: Mechanics and Material Engineering*, 38, 458-464.

Todoroki, A. and Yoshida, J. (2004). Electrical resistance change of unidirectional CFRP due to applied load. *JSME International Journal, Series A: Solid Mechanics and Material Engineering*, 47, 357-364.

Todoroki, A. and Yoshida, J. (2005). Apparent negative piezoresistance of single-ply CFRP due to poor electrical contact of four-probe method. *Key Engineering Materials*, 297-300, 610-615.

Ueda, M. and Todoroki, A. (2006). Asymmetrical dual charge EPCM for delamination monitoring of CFRP laminate. *Key Engineering Materials*, 321-323, 1309-1315.

Ueda, M. and Todoroki, A. (2008). Delamination monitoring of CFRP laminate using the two-stage electric potential change method with equivalent electric conductivity. *Engineering Fracture Mechanics*, 75, 2737-2750.

Ueda, M., Todoroki, A., Shimamura, Y., and Kobayashi, H. (2004). Monitoring delamination of laminated CFRP using the electric potential change method: Application of normalization method and the effect of the shape of a delamination crack. *Advanced Composite Materials: The Official Journal of the Japan Society of Composite Materials*, 13, 311-324.

Ueda, M., Todoroki, A., Shimamura, Y., and Kobayashi, H. (2005). Monitoring delamination of laminated CFRP using the electric potential change method (two-stage monitoring for robust estimation). *Advanced Composite Materials: The Official Journal of the Japan Society of Composite Materials*, 14, 83-97.

Wang, S. and Chung, D. D. L. (2000). Piezoresistivity in continuous carbon fiber polymer-matrix composite. *Polymer Composites*, 21, 13-19.

Welch, W. J., Buck, R. J., Sacks, J., Wynn, H. P., Mitchell, T. J., and Morris, M. D. (1992). Screening, predicting, and computer experiments. *Technometrics*, 34, 15-25.

Xia, Z., Okabe, T., Park, J. B., Curtin, W. A., and Takeda, N. (2003). Quantitative damage detection in CFRP composites: coupled mechanical and electrical models. *Composites Science and Technology*, 63, 1411-1422.

Xu, M. X., Liu, W. G., Gao, Z. X., Fang, L. P., and De Yao, K. (1996). Correlation of change in electrical resistance with strain of carbon fiber-reinforced plastic in tension. *Journal of Applied Polymer Science*, 60, 1595-1599.

Yamazaki, K. (1996). Two-level optimization technique of composite laminate panels by genetic algorithms. *Proceedings of the 1996 37th AIAA/ASME/ASCE/AHS/ASC Structures, Structural Dynamics, and Materials Conference Part 4*, Salt Lake City, UT. pp. 1882-1887.

Zako, M., Takano, N., Takeda, N., and Tsujikami, T. (1997). Cost effective design procedure for laminated composite structure based on GA. *Science and Engineering of Composite Materials*, 6, 131-140.